Nanoscale

ROYAL SOCIETY OF CHEMISTRY

COMMUNICATION

View Article Online
View Journal | View Issue

Cite this: *Nanoscale*, 2024, **16**, 3417

Received 25th October 2023,
Accepted 2nd January 2024

DOI: 10.1039/d3nr05387c

rsc.li/nanoscale

One-step regeneration and upgrading of spent $LiFePO_4$ cathodes with phytic acid†

Xuhui Zhu, Xueqi Ren, Junting Chen, Mengqi Gong, Ran Mo, Siyuan Luo and Shun Yang *

The regeneration and upgrading of spent $LiFePO_4$ cathodes (S-LFP) were achieved *via* a one-step hydrothermal treatment. The reducing effect of phytic acid could restore the degraded structure associated with an aqueous Li source. Meanwhile, Li ions are easily chelated by phytic acid groups, and a Li_3PO_4 coating layer could be formed to reconstruct the surface of the LFP. The regenerated LFP exhibits faster reaction kinetics, larger high-rate charge/discharge capacity, and better cycling performance than commercial LFPs, suggesting that our proposed strategy is a promising technology for the recovery of spent cathode materials.

With the accelerating development of the lithium-ion battery (LIB) industry, a large amount of spent LIBs will be generated at their end-in-life.[1–3] The hazardous organics and heavy metals in the spent LIBs will be a heavy burden on the environment. The improper treatment of spent LIBs will also lead to a huge waste of valuable metal resources.[4,5]

Pyrometallurgical and hydrometallurgical technologies have been widely adopted to recover valuable metals from the spent LIBs. However, pyrometallurgical and hydrometallurgical processes involve huge energy consumption, waste chemicals, and complex steps.[6–8] The cathode loses a significant portion of its value after the destructive treatment of these two recovery processes, leading to low economic benefits, especially for some cathodes that do not contain valuable metals (Ni and Co), such as $LiFePO_4$ (LFP).[9,10] Recently, direct cathode regeneration has been highlighted to recycle spent $LiFePO_4$ (S-LFP) cathodes, owing to its less energy consumption, convenient operation, and higher economic profits.[11–14] In previous reports, solid-state sintering, hydrothermal treatment, and chemical lithiation have been proposed for the direct regeneration of S-LFP, and an effective reductive environment is considered very important for the elimination of Fe(III) and Li–Fe anti-site defects in the crystal structure of S-LFP.[15–18]

Moreover, sluggish charge transport and poor cycling stability are inherent disadvantages of LFP cathode materials, which directly hinder their practical applications.[19,20] Surface modification is widely adopted to improve the electrochemical performance of LFP.[21–23] Therefore, reducing and extra functional agents need to be added to restore the degraded crystal structure and even upcycle the electrochemical performance by modifying the LFP surface. Phosphates are widely used in the modification of cathode materials, in which the doping phosphorus (P) has been reported to enhance electronic conductivity. Moreover, the polyanion $(PO_4)^{3-}$ could chemically stabilize the transition metal ions, and the formed compound, such as Li_3PO_4 could improve electrochemical stability at high potential and improve lithium-ion transport.[24–27]

Herein, phytic acid, as a natural and nontoxic organic large molecular compound, existing in plants and commonly used in industry as an antioxidant and polydentate metal chelating, is adopted to restore S-LFP and construct functional layers on

School of Chemistry and Materials Science, Jiangsu Normal University, Xuzhou, Jiangsu, 221116, China. E-mail: yangshun@jsnu.edu.cn

†Electronic supplementary information (ESI) available. See DOI: https://doi.org/10.1039/d3nr05387c

Shun Yang

Dr Shun Yang obtained his BS degree in material chemistry from the University of Jinan (2011), and received his PhD in applied chemistry from Soochow University under the supervision of Prof. Jianmei Lu in (2016). He has been an associate professor in the School of Chemistry and Materials Science at Jiangsu Normal University in Xuzhou, China since 2016. His current research interests include recycling of spent lithium-ion batteries and novel nanocomposites for biomedical applications and wastewater remediation.

the surface of regenerated LFP (R-LFP) for upgrading the electrochemical performance, simultaneously. In the hydrothermal treatment process, phytic acid with strong reductive properties could decrease the amount of Fe(III) in S-LFP,[28,29] and aqueous Li source could fill the vacancies to restore the degraded crystal structure. Meanwhile, Li ions are easily chelated by phytic acid groups, and a Li_3PO_4 coating layer could be formed under high temperature and pressure to reconstruct the surface of R-LFP (R-LFP-LP). The regeneration and upgrading of S-LFP are simultaneously realized in one step (Fig. 1a). The electrochemical performance of R-LFP-LP cathode is fully restored and even upcycled, and superior to that of commercial LFP owing to the functional Li_3PO_4 coating. Our proposed strategy opens up opportunities for future recycling and upgrading of spent LIBs.

The S-LFP cathode powder was obtained from spent 18 650 batteries after the discharge, and manual dismantling and separation of Al foil (Fig. S1†). In the restoring process, S-LFP was dispersed in an aqueous solution containing phytic acid and LiOH, and the mixture was transferred to a Teflon liner autoclave for the hydrothermal treatment. To verify the change in phase composition, X-ray powder diffraction (XRD) was conducted (Fig. 1b), and the results showed the existence of the $FePO_4$ phase in S-LFP, and the $FePO_4$ phase disappeared after the hydrothermal treatment, indicating that Fe(III) could be reduced by the reductive phytic acid. In addition, a new phase corresponding to Li_3PO_4 was observed in the XRD spectrum after the hydrothermal treatment, and the product was denoted as Li_3PO_4 coating regenerated LFP (R-LFP-LP). To further confirm the formation of Li_3PO_4, a mixture of phytic acid and LiOH in water was subjected to a hydrothermal reaction, the XRD pattern of the precipitate, as shown in Fig. S2,† demonstrated that Li_3PO_4 could be formed in the hydrothermal process. As previously reported, the Li–Fe anti-site defects in the S-LFP structure could be eliminated under a reducing atmosphere, Rietveld refinement was performed on the full XRD data of S-LFP (Fig. 1c and Table S1†) and R-LFP-LP (Fig. 1d and Table S2†) to confirm this phenomenon. The content of Fe–Li defects in S-LFP was calculated to be ~6.10%, and this value decreased to only ~2.20% in R-LFP-LP, further demonstrating that the degraded structure of S-LFP was fully restored. Moreover, Fe–Li defects also could be qualified by Fourier transform infrared (FTIR) spectroscopy. In the FTIR spectra of S-LFP and R-LFP-LP (Fig. 1e), the peak at ~970.67 cm^{-1} in S-LFP corresponding to the Fe–Li defect shifted to a lower wavenumber (~969.31 cm^{-1}) in R-LFP-LP, indicating the decrease of Fe–Li defects. The valence state of the Fe was also studied by X-ray photoelectron spectroscopy (XPS) (Fig. 1f and S3†), and the Fe(III) phase could be observed in both, the high resolution of Fe $2p_{3/2}$ and Fe $2p_{1/2}$ in S-LFP. However, the Fe(III) phase disappeared in R-LFP-LP, indicating that the FP phase was completely eliminated after the restoring process. The contents of Fe and Li were studied by inductively coupled plasma-optical emission spectrometry (ICP-OES) (Fig. 1g). The loss of lithium is the dominant reason for the degradation of S-LFP, and the Li/Fe molar ratio in S-LFP was only 0.67, the value increased to 1.15 in R-LFP-LP, indicating the full restoration of the structure and composition in LFP. The Raman spectra of S-LFP and R-LFP-LP were measured (Fig. S4†), and new narrow peaks corresponding to LFP appeared in the spectrum of R-LFP-LP, confirming that the crystallization of the cathode particles was improved.[30]

Scanning electron microscope (SEM) images of S-LFP and R-LFP-LP particles (Fig. S5†) showed that the particle size did not change after the hydrothermal treatment, but the surface of R-LFP-LP became more smooth. The microstructure of S-LFP and R-LFP-LP particles were studied using high-resolution TEM (HRTEM). A thin and discontinuous carbon layer on the surface of S-LFP was observed, as shown in Fig. 2a. Three areas in the S-LFP were selected to analyse the crystal structure in detail. As shown in Fig. 2b, both the disordered area and FFT images indicated the degradation of the crystal structure of S-LFP. Fig. 2c and d show the $FePO_4$ phase with (021) crystal plane (interplanar spacing of 0.344 nm) and (020) crystal plane

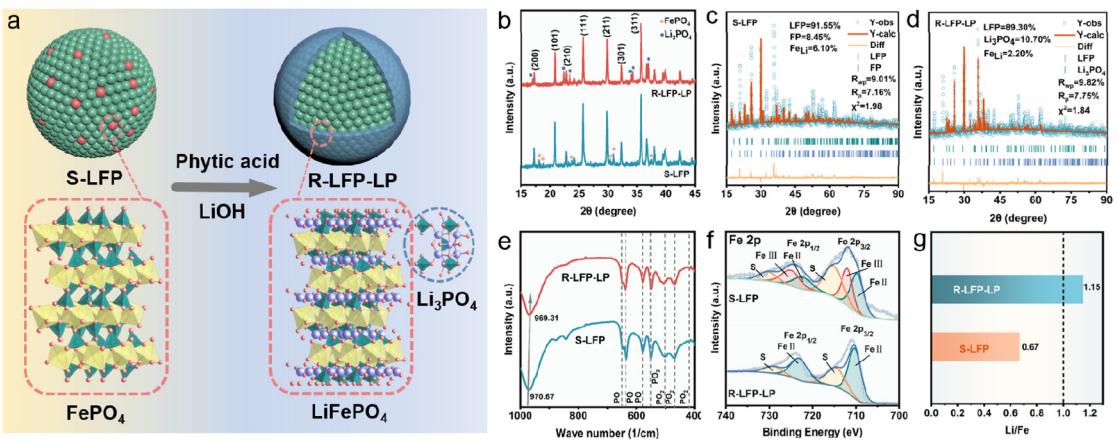

Fig. 1 (a) Schematic illustration of the regeneration process. (b) XRD patterns of S-LFP and R-LFP-LP. Rietveld refinement results of (c) S-LFP and (d) R-LFP-LP. (e) FTIR of S-LFP and R-LFP-LP. (f) High-resolution XPS spectra of Fe 2p. (g) Li/Fe molar ratio in S-LFP and R-LFP-LP.

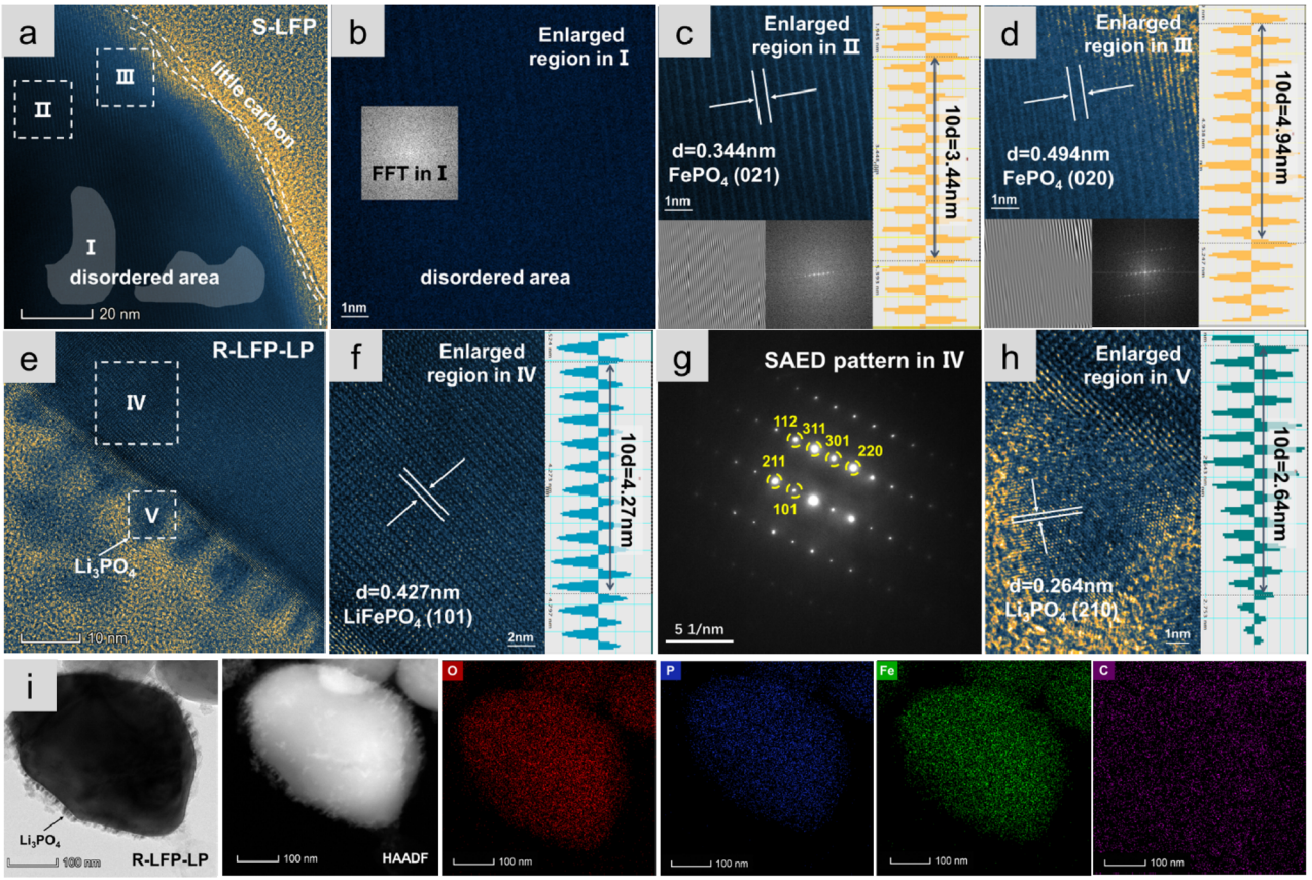

Fig. 2 (a) HRTEM image, (b–d) enlarged figures, corresponding line profiles, and FFT images of S-LFP. (e) HRTEM image, (f and h) enlarged figures, the corresponding line profiles, (g) SAED pattern of R-LFP-LP. (i) TEM mapping images of R-LFP-LP.

(interplanar spacing of 0.494 nm). The FFT images insets of Fig. 2c and d also confirmed the existence of the $FePO_4$, which is consistent with the above results. For R-LFP-LP, some particles were observed on the surface of the R-LFP-LP (Fig. 2e), and two areas in the bulk and surface of the LFP particle were selected. As shown in Fig. 2f, the (101) crystal plane of $LiFePO_4$ with an interplanar spacing of 0.427 nm in the bulk structure confirmed that the crystal structure of LFP was restored. Moreover, the structure was studied by selected area electron diffraction (SEAD) (Fig. 2g), and the pattern showed dark and bright spots, which can be indexed to the $LiFePO_4$, confirming that the LFP crystal structure is highly crystalline in order.

Fig. 2h shows an enlarged image of the small particles on the surface of R-LFP-LP; the (210) crystal plane of Li_3PO_4 with interplanar spacing of 0.264 nm proved the successful coating of the Li_3PO_4 layer, and the thickness of the Li_3PO_4 nanolayer was estimated at approximately 9.6 nm, which was beneficial for improving the electrochemical performance. Moreover, the content of Li_3PO_4 in R-LFP-LP was about 10.70% according to the Rietveld refinement analyses of XRD (Table S2†). Compared with S-LFP (Fig. S6†), the TEM image of R-LFP-LP shown in Fig. 2i also confirmed the appearance of Li_3PO_4, and highly spatially resolved TEM mapping showed the uniform distribution of the elements Fe, N, C, O, and P. The above results all supported the full restoration of the crystal structure of S-LFP and the successful coating of Li_3PO_4.

The discharge specific capacity at 1C (1C = 170 mA g^{-1}) of the S-LFP, R-LFP-LP, and commercial LFP (C-LFP) were 75.9, 143.9, and 138.5 mA h g^{-1}, respectively (Fig. 3a). The highest capacity of R-LFP-LP indicated that the electrochemical performance was recovered and upgraded. The reversibility of the Li-ion insertion and extraction kinetics of S-LFP, R-LFP-LP, and C-LFP were studied by cyclic voltammetry (CV) experiments at a scan rate of 0.1 mV s^{-1} (Fig. 3b–d). It could be observed that R-LFP-LP has the smallest potential interval (217 mV) between the reduction and oxidation peaks, indicating that the blocked channel for Li ion insertion and extraction caused by Fe–Li defects was repaired, and Li_3PO_4 on the surface could improve lithium ion transport. The charge transfer kinetics were also studied by electrochemical impedance spectroscopy (EIS), and the equivalent circuit is shown in Fig. 3e, the charge transfer resistance (R_{ct}) of R-LFP-LP was smaller than that of C-LFP. The Li-ion diffusion coefficient (D_{Li^+}) could be further calculated by linear fitting of the relation plot between Z' and the reciprocal square root of the angular frequency ω (Fig. S7†),[31] the D_{Li^+} values of S-LFP, R-LFP-LP, and C-LFP were 6.51×10^{-16} cm^2 s^{-1}, 1.27×10^{-15} cm^2 s^{-1}, and 9.02×10^{-16} cm^2 s^{-1}, respectively. Moreover, the D_{Li^+} of S-LFP, R-LFP-LP and C-LFP

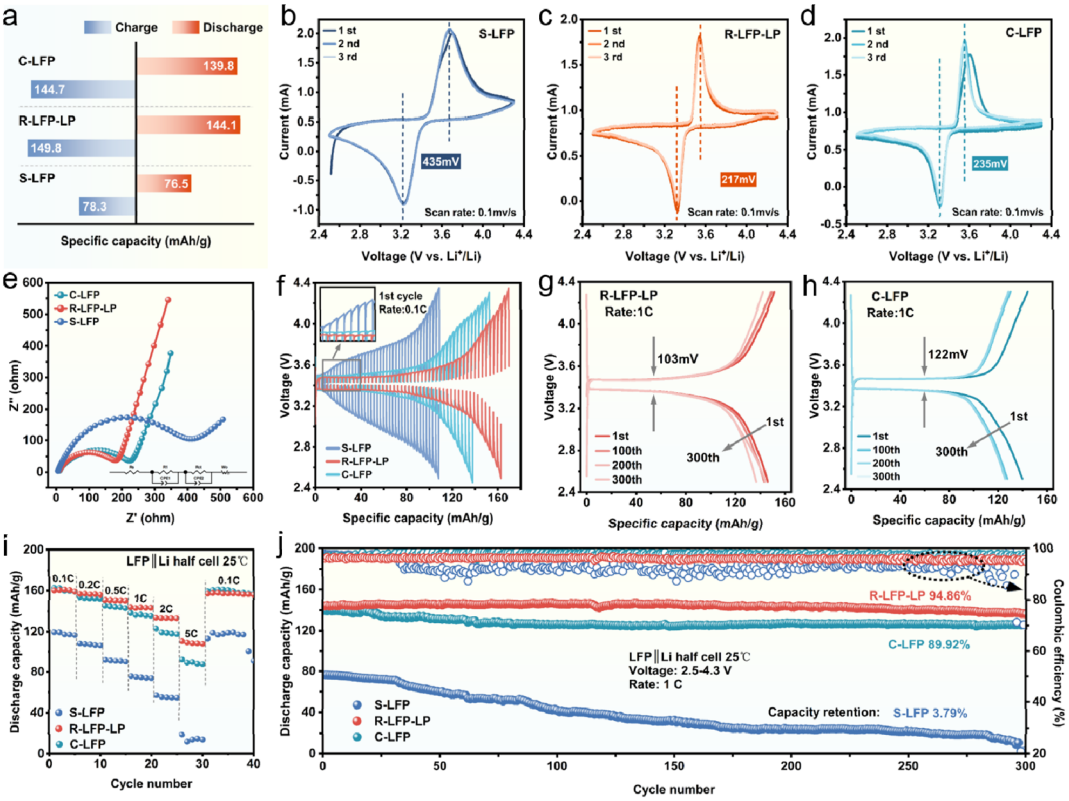

Fig. 3 (a) The restored capacity at 1C. (b–d) CV curves with a scan rate of 0.1 mV s^{-1}. (e) Nyquist plots of the cathodes. (f) Charge and discharge voltage profiles from the GITT plots at 0.1C. Galvanostatic charge/discharge profiles of the (g) R-LFP-LP and (h) C-LFP at 1C. (i) Rate performance and (j) cycling performance of the LFP cathodes.

were also measured using the galvanostatic intermittent titration technique (GITT) (Fig. 3f and S8†), and the values were 8.22×10^{-13} cm^2 s^{-1}, 3.90×10^{-12} cm^2 s^{-1}, and 2.34×10^{-12} cm^2 s^{-1}, respectively. EIS reflects the rate of Li^+ diffusion within the active substance, whereas, in the GITT method, it is considered that the diffusion process occurs mainly on the surface layer of the particle.[32,33] Both, the EIS and GITT results confirmed that the Li_3PO_4 coated cathode materials had faster lithiation and de-lithiation kinetics than C-LFP. In addition, the polarization voltage of R-LFP-LP remained low as the number of cycles increased and was only 103 mV after 300 cycles (Fig. 3g), which was smaller than that of C-LFP (122 mV) (Fig. 3h), also demonstrating that R-LFP-LP had faster kinetics than C-LFP.

Fig. 3i shows the rate capability of S-LFP, R-LFP-LP, and C-LFP. S-LFP exhibited the worst performance due to the degraded structure, and the discharge capacities of R-LFP-LP were similar to those of C-LFP at low current densities. However, the discharge capacities of R-LFP-LP were 133.6 mA h g^{-1} and 106 mA h g^{-1} at 2C and 5C, respectively, which are much higher than those of C-LFP. In addition, the long-term cycling performance of R-LFP-LP, C-LFP, and S-LFP samples at 1C within a voltage range of 2.0–4.8 V is presented in Fig. 3j. The capacity retention for the S-LFP cathode at 1C was only 3.79% after 300 cycles, and the R-LFP-LP showed excellent cycling stability with a capacity retention of 94.86%. It is worth noting that the capacity retention of R-LFP-LP was also higher than that of the C-LFP (89.92%). Moreover, the stability of R-LFP-LP was studied by SEM, the invisible changes in the surface of R-LFP-LP before and after long-term cycling confirmed the good stability of R-LFP-LP (Fig. S9†). From the above results, it could be concluded that after hydrothermal treatment with phytic acid, the electrochemical performance of S-LFP was fully recovered. The introduction of Li_3PO_4 could further improve the reaction kinetics, and P–O could also stabilize the Fe ions to improve the rate capability and cycling performance. Therefore, the spent $LiFePO_4$ cathodes was regenerated and upgraded in a one-step reaction.

Conclusions

In conclusion, the S-LFP cathode materials were regenerated and upgraded by phytic acid in a one-step hydrothermal treatment. Comprehensive structural characterizations demonstrated the degraded structure of S-LFP was fully restored under the reducing effect of phytic acid associated with the aqueous Li source, and a Li_3PO_4 coating layer was formed on the surface of LFP during this process, simultaneously. The electrochemical measurements showed that the electrochemical performance of the S-LFP was not only fully recovered, but was also upgraded by the Li_3PO_4 coating layer, and R-LFP-LP exhibited faster reaction kinetics, larger high-rate

charge/discharge capacity, and better cycling performance compared with C-LFP. All these advantages demonstrated that our strategy had excellent flexibility and potential for the recovery of spent $LiFePO_4$ cathodes.

Author contributions

X. Z. and S. Y. conceived the project. X. Z. fabricated the samples, performed electrochemical measurements, and analysed the data with the assistance of X. R., J. C., M. G., R. M., and S. L. All authors discussed and contributed to the results. S. Y. supervised the research and wrote the manuscript with comments and revisions from all the authors.

Conflicts of interest

There are no conflicts to declare.

Acknowledgements

We gratefully acknowledge the financial support provided National Natural Science Foundation of China (51802127), the Postgraduate Research and Practice Innovation Program of Jiangsu Province (KYCX22_2784).

References

1 Y. S. Tian, G. B. Zeng, A. Rutt, T. Shi, H. Kim, J. Wang, J. Koettgen, Y. Sun, B. Ouyang, T. N. Chen, Z. Y. Lun, Z. Q. Rong, K. Persson and G. Ceder, *Chem. Rev.*, 2021, **121**, 1623–1669.
2 Z. J. Baum, R. E. Bird, X. Yu and J. Ma, *ACS Energy Lett.*, 2022, **7**, 712–719.
3 J. Wu, M. Zheng, T. Liu, Y. Wang, Y. Liu, J. Nai, L. Zhang, S. Zhang and X. Tao, *Energy Storage Mater.*, 2023, **54**, 120–134.
4 G. Harper, R. Sommerville, E. Kendrick, L. Driscoll, P. Slater, R. Stolkin, A. Walton, P. Christensen, O. Heidrich, S. Lambert, A. Abbott, K. Ryder, L. Gaines and P. Anderson, *Nature*, 2019, **575**, 75–86.
5 P. Xu, Q. Dai, H. Gao, H. Liu, M. Zhang, M. Li, Y. Chen, K. An, Y. S. Meng, P. Liu, Y. Li, J. S. Spangenberger, L. Gaines, J. Lu and Z. Chen, *Joule*, 2020, **4**, 2609–2626.
6 R. E. Ciez and J. F. Whitacre, *Nat. Sustainability*, 2019, **2**, 148–156.
7 G. Qian, Z. Li, Y. Wang, X. Xie, Y. He, J. Li, Y. Zhu, S. Xie, Z. Cheng, H. Che, Y. Shen, L. Chen, X. Huang, P. Pianetta, Z. Ma, Y. Liu and L. Li, *Cell Rep. Phys. Sci.*, 2022, **3**, 100741.
8 X. H. Zhu, Y. J. Li, M. Q. Gong, R. Mo, S. Y. Luo, X. Yan and S. Yang, *Angew. Chem., Int. Ed.*, 2023, **62**, e202300074.
9 G. Ji, J. Wang, Z. Liang, K. Jia, J. Ma, Z. Zhuang, G. Zhou and H. Cheng, *Nat. Commun.*, 2023, **14**, 584.
10 K. Jia, J. Ma, J. Wang, Z. Liang, G. Ji, Z. Piao, R. Gao, Y. Zhu, Z. Zhuang, G. Zhou and H. Cheng, *Adv. Mater.*, 2022, **35**, 2208034.
11 M. Fan, Q. Meng, X. Chang, C. Gu, X. Meng, Y. Yin, H. Li, L. Wan and Y. Guo, *Adv. Energy Mater.*, 2022, **12**, 2103630.
12 J. Chen, Q. Li, J. Song, D. Song, L. Zhang and X. Shi, *Green Chem.*, 2016, **18**, 2500–2506.
13 T. Ouaneche, M. Courty, L. Stievano, L. Monconduit, C. Guéry, T. M. Sougrati and N. Recham, *J. Power Sources*, 2023, **579**, 233248.
14 X. Tang, R. Wang, Y. Ren, J. Duan, J. Li and P. Li, *J. Mater. Sci.*, 2020, **55**, 13036–13048.
15 X. Xiao, L. Wang, Y. Wu, Y. Song, Z. Chen and X. He, *Energy Environ. Sci.*, 2023, **16**, 2856–2868.
16 Q. Liang, H. Yue, S. Wang, S. Yang, K. Lam and X. Hou, *Electrochim. Acta*, 2020, **330**, 135323.
17 C. Wu, J. Hu, L. Ye, Z. Su, X. Fang, X. Zhu, L. Zhuang, X. Ai, H. Yang and J. Qian, *ACS Sustainable Chem. Eng.*, 2021, **9**, 16384–16393.
18 K. Park, J. Yu, J. Coyle, Q. Dai, S. Frisco, M. Zhou and A. Burrell, *ACS Sustainable Chem. Eng.*, 2021, **9**, 8214–8221.
19 W. B. Luo, S. L. Chou, Y. C. Zhai and H. K. Liu, *J. Mater. Chem. A*, 2014, **2**, 4927–4931.
20 Q. Q. Xiong, J. J. Lou, X. J. Teng, X. X. Lu, S. Y. Liu, H. Z. Chi and Z. G. Ji, *J. Alloys Compd.*, 2018, **743**, 377–382.
21 G. L. Cai, R. S. Guo, L. Liu, Y. X. Yang, C. Zhang, C. Wu, W. N. Guo and H. Jiang, *J. Power Sources*, 2015, **288**, 136–144.
22 X. F. Wang, Z. J. Feng, J. T. Huang, W. Deng, X. B. Li, H. S. Zhang and Z. H. Wen, *Carbon*, 2018, **127**, 149–157.
23 J. Sun, Z. Jiang, P. Jia, S. Li, W. Wang, Z. Song, Y. Mao, X. Zhao and B. Zhou, *Waste Manage.*, 2023, **158**, 125–135.
24 L. Yi, H. Jiang and K. Liang, *Ceram. Int.*, 2022, **48**, 3374–3382.
25 Z. Wang, H. Zhao, B. Zhou, J. Li, Y. Qi, K. Liang, Q. Zhao, Z. Ding and Y. Ren, *ACS Appl. Energy Mater.*, 2023, **6**, 387–396.
26 Z. Chen, G. T. Kim, D. Bresser, T. Diemant, J. Asenbauer, S. Jeong, M. Copley, R. J. Behm, J. Lin, Z. Shen and S. Passerini, *Adv. Energy Mater.*, 2018, **8**, 1801573.
27 Q. Gan, H. He, Y. Zhu, Z. Wang, N. Qin, S. Gu, Z. Li, W. Luo and Z. Lu, *ACS Nano*, 2019, **13**, 9247–9258.
28 F. Zhang, N. Qin, Y. Li, H. Guo, Q. Gan, C. Zeng, Z. Li, Z. Wang, R. Wang, G. Liu, S. Gu, H. Huang, Z. Yang, J. Wang, Y. Deng and Z. Lu, *Energy Environ. Sci.*, 2023, **16**, 4345–4355.
29 M. Cheryan and J. J. Rackis, *Crit. Rev. Food Sci. Nutr.*, 1980, **13**, 297–335.
30 Z. Lazarević, G. Križan, J. Križan, A. Milutinović, M. Gilić, I. Kuryliszyn-Kudelska and N. Romčević, *Sci. Sintering*, 2019, **51**, 309–318.
31 Q. Zhao, Y. Zhang, Y. Meng, Y. Wang, J. Ou, Y. Guo and D. Xiao, *Nano Energy*, 2017, **34**, 408–420.
32 T. Q. Nguyen and C. Breitkopf, *J. Electrochem. Soc.*, 2018, **165**, E826.
33 Z. Shen, L. Cao, C. D. Rahn and C. Y. Wang, *J. Electrochem. Soc.*, 2013, **160**, A1842.